

TiO₂를 첨가한 산화 아연 바리스터에 대한 열자극전류의 기원

The Origin of Thermally Stimulated Current in Zinc Oxide Varistors with TiO₂ Additions

장경욱*, 이성일**, 이준웅***
(Kyung-Uk Jang, Sung-Il Lee, Joon-Ung Lee)

요 약

ZnO 바리스터의 비선형 전도특성은 입자의 구조로부터 설명할 수 있다. 본 논문에서는 ZnO 바리스터의 입자구조에 트랩된 캐리어를 분석하기 위해서 TSC 측정 기법을 사용하였다. 측정 결과로부터, 네개의 TSC피크를 얻었다.

고온으로부터, 첫번째, 두번째와 세번째 TSC피크의 기원은 각각 트랩, 도너 밀도 및 입계층의 트랩으로 나타나고, 네번째 피크의 기원은 공핍층에 있는 도너 이온의 탈분극에 의해서 기인하는 것으로 사료된다. α_1 피크의 활성화 에너지는 약 0.33~1.42 eV였다. 또한, 바리스터의 예비동작 영역에서의 전도특성은 α_1 과 α_2 피크의 값에 지배된다는 것을 확인 하였다.

Abstract

The mechanism of non-linear conduction of ZnO varistors may be explained on the basis of the grain structure. In this paper, the TSC spectrum was measured to study the trapped carriers in grain structure of ZnO varistors.

From the result of measurement, four peaks of TSC may be distinguished on the obtained spectrum of TSC. The origin of the first, second and third TSC peaks appeared from the high temperature was trap, donor level and deep trap, respectively. The origin of the fourth peak was attributed to the process of depolarization of the donor ions in the depletion layer. The activation energy of α_1 peak is about 0.33~1.42 eV. The conduction properties in prebreakdown region for ZnO varistor may be determined by the height of α_1 and α_2 peak.

1. Introduction

The ZnO varistor has an very excellent non-linearity and a large surge-energy absorption capability. For these reasons, zinc oxide varistors are often used in low voltage circuits such as electronic circuit-

* 광운대학교 대학원 전기공학과

** 충주 산업대학 산업안전공학과

*** 광운대학교 공과대학 전기공학과

接受日字:1992년 9월 21일

ts. To particularly reduce the breakdown voltage of ZnO varistors, it is required to produce the samples with some concentration of additions[2,8]. The line voltage following the ZnO varistor is continuously applied to the varistor because of the gapless arrestor, so that the leakage current, though it is very small, flows through it. The leakage current gradually increases as the degradation of the varistor proceeds[1].

The electrical properties of ZnO varistors greatly depend on the grain structure of ZnO. The mechanism of non-linear conduction of ZnO varistors can be explained by the basis of the grain structure. Some researchers[3,4] proposed the band model, based on the double Schottky barriers, to explain the conduction and degradation mechanism in zinc oxide varistors. However, the conduction and degradation mechanism in zinc oxide varistors still is not completely reasonable mechanism in ZnO varistors. Accordingly, this paper presents the results of the investigation of the thermally stimulated current in the low voltage zinc oxide varistors with TiO_2 additives as follows: The TSC measurement of the ZnO varistors with TiO_2 as additives was conducted in order to obtain the equivalent model for the conduction and degradation mechanism of low voltage varistors, and the results of the investigation are presented. In particular, the spectra of TSC are measured in the temperature range of $-130 \sim 200^\circ\text{C}$ with a various forming electric fields E_f , temperature T_f .

Four peaks of TSC may be clearly distinguished on the obtained spectrum of TSC. It is namely observed that there are appeared the peaks of α_1 , α_2 , β and γ from high temperature in a TSC spectrum.

It seems that α_1 peak is due to depolarization of donor ions forming the space charge in the depletion layer, and α_2 peak is due to the detrapping of trapped electrons in deep trap level of intergranular layer, and β peak is due to the thermal exciting of carrier existing in the donor level of grain itself, and γ peak is due to the thermal exciting of

trapped carrier in all of shallow trap site distributed the inner of sample and/or a intrinsic impurity existing in it.

2. Experimental Procedure and TSC Measurement

The powder of varistor were used chemically reagents of 99.9% purity.

All ZnO ceramic samples were prepared by the same procedure with acetone of

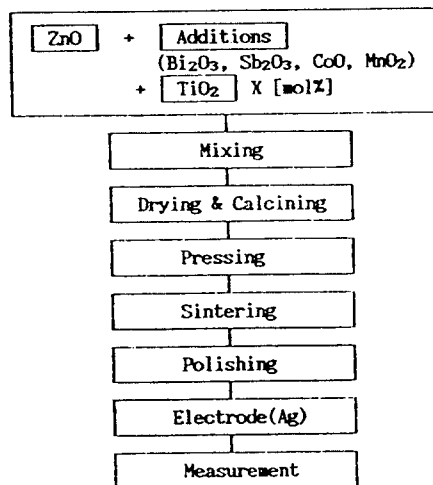


Fig. 1 Simplified flow diagram for fabrication of ZnO varistors.

50 wt% as shown in Fig. 1. The main components of ZnO ceramic sample were ZnO (97-x mol%) and such additives as Sb_2O_3 (1 mol%), Bi_2O_3 (1 mol%), CoO (0.5 mol%) and MnO_2 (0.5 mol%). These components (x=0 mol%) were mixed, and created one type of specimen reagent was created by adding TiO_2 (x=2 mol%) to the previous mixed components.

The above mixtures (raw material) was calcined for two hours at the temperature of 750°C , and then the calcined powders were made granular and sieved with 120 mesh. Polyvinylalcohol (PVA) was used as the binder in this process. The mixture was pressed at 400 kg/cm^2 into discs type and sintered for two hours at the temperature of 1300°C in the air. Both sides of the sintered discs were polished with SiC powder. Later, both surfaces of the polished discs were metallized with silver paste, which served as conducting electrodes. The

specimen in final stage was 12mm in diameter and 1mm in thickness. Fig.1 presents the simplified flow diagram of the ZnO varistors fabrication process used in the investigation.

A block diagram of TSC equipment is shown in Fig. 2. As shown in Fig. 2, the equipment consists of main body, current measuring unit, DC power supply unit, X-T recorder and thermal controlled.

Before the measurement of TSC spectrum was conducted, the tested samples were formed under the following conditions: the forming electric field was in the range of 2-6kV/m and the forming temperature was 50 °C for forming time equal of 5min. The TSC spectrum was taken by increasing the temperature in the range from - 150°C to 200°C. The temperature of the sample was raised at a rate of 5°C/min.

3. Results and Discussion

The TSC of ZnO varistor was reported to be caused by the emission of trapped carriers existed in the bulk [7]. When thermally stimulated currents arise as the emission of trapped carriers, the decays of total charges by trapped carriers may be expressed as follows:(9)

$$\frac{dq}{dt} = - \frac{q}{\tau} \quad (1)$$

where q is the total charge of trapped carriers and τ is the relaxation time.

For the constant rate of heating, the charge may be calculated from equation and is equal:

$$q = q_0 \exp \left[- \int_{T_0}^T dt / \tau \right] \quad (2)$$

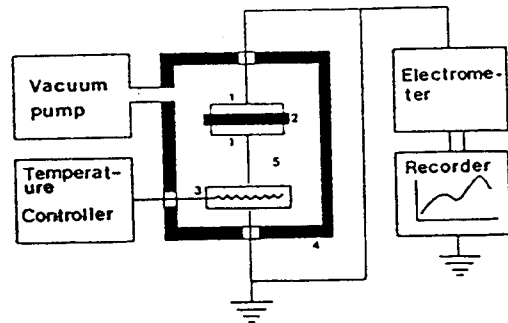
where q_0 is the charge at the initial temperature T_0 .

The relaxation time τ at various temperatures depends on the activation energy and is represented by equation(3):

$$\tau = \tau_0 \exp(E_t/kT) \quad (3)$$

where, E_t : activation energy
 k : Boltzmann's constant
 T : absolute temperature

On the other hand, the TSC spectrum $I(T)$ is equal:



1 Electrode 2 Specimen 3 Heater
 4 Oven 5 Dry N₂ Gas

Fig.2 Schematic Diagram of TSC Measuring Apparatus.

$$I(T) = - dq/dt = I_0 \exp(-E_t/kT) \exp[-1/\tau_0 \beta \int_{T_0}^T \exp(E_t/kT') dT'] \quad (4)$$

where, I_0 ($= q_0/\tau_0$) is the physical quantity described in paper, and due to the initial charge quantity in the sample without electrical field(4), [10].

At low temperature, the $I(T)$ function given in Equation (4) may be expressed:

$$\ln I(T) = \ln I_0 - E_t/kT \quad (5)$$

On the other hand, applying the condition for the maximum value, $dI/dT = 0$, to eq. (4), eq. (6) is derived

$$\frac{H}{kT_m^2} = \frac{I}{\beta \tau_0} = \exp \left(- \frac{H}{kT_m} \right) \quad (6)$$

τ is calculated from activation energy as follows.

$$\tau(T) = \tau_0 \exp \left(- \frac{H}{kT} \right) = \left[\frac{kT_m^2}{H\beta} \exp \left(- \frac{H}{kT_m} \right) \right] \exp \left(\frac{H}{kT} \right) \quad (7)$$

If forming time is sufficiently long and $\mu_d E_t/kT_f \ll 1$, initial total charge quantity is derived to eq. (8). μ_d is the mobility of carriers being depleted region

$$q_0 = \frac{N_d \mu_d^2}{3kT_f} E_f \quad (8)$$

As a result of above equations, $I(T)$ of TSC is that

$$I(T) = \frac{N_d \mu_d^2}{3kT_f \tau_o} E_f \exp(-H/kT) \exp \left[\frac{-1}{\tau_o \beta} \int_{T_o}^T \exp(H/kT') dT' \right] \quad (9)$$

Therefore, from the result of measurement, the quantity of q become eq. (10).

$$q(T) = \frac{N_d \mu_d^2}{3kT_f} E_f \exp(-H/kT) \exp \left[\frac{-1}{\tau_o \beta} \int_{T_o}^T \exp(H/kT') dT' \right] \quad (10)$$

The charge quantity of Q_{TSC} is obtained from the integral of TSC peak,

$$Q_{TSC} = \frac{N_d \mu_d^2}{3kT_f} E_f \alpha E_f \quad (11)$$

where N_d is the density of carrier and μ_d the mobility of carrier in depletion layer and trap state.

The activation energy H may be determined from the diagram of $\ln I(T)$ versus $1/T$. The relationship of $\ln I(T)$ versus $1/T$ is presented in Fig.3 through Fig.6. The activation energy calculated by this method is presented in Table 1.

Fig.3 and fig.4 show the TSC spectrum for samples without TiO_2 and samples with 2 mol% TiO_2 which is formed electric at temperature 50°C during 5 min, and at

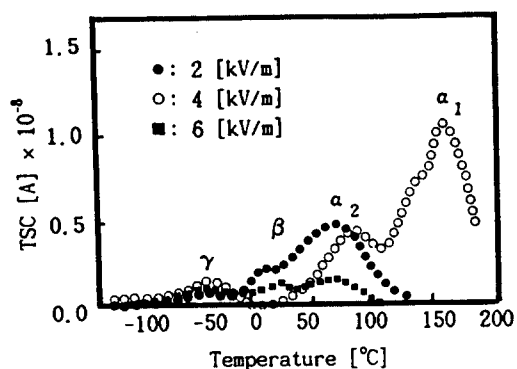


Fig.3 TSC spectrum of ZnO varistors without TiO_2 ,
various forming electrical field:
2, 4 and 6[V],
forming temperature:50[°C],
forming time:5[min.]
rising time:5[°C/min.]

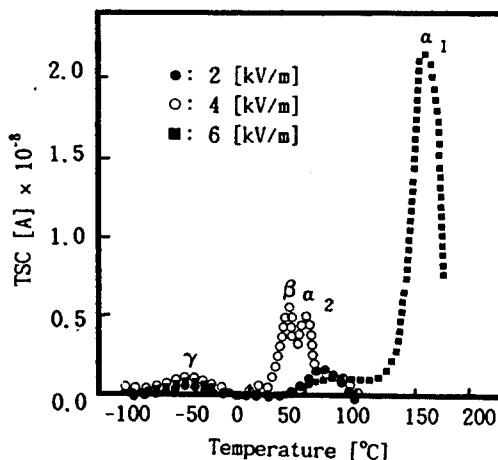


Fig.4 TSC spectrum of ZnO varistors with TiO_2 2 mol%,
various forming electrical field:
2, 4 and 6[V],
forming temperature:50[°C]
forming time:5[min.]
rising time:5[°C/min.]

forming electric field 2, 4 and 6 kV/m. On these figures of the TSC spectrum may be observed four peaks which are labeled as α_1 , α_2 , β and γ from the higher temperature.

The γ , β , and α_2 peaks appeared at all forming electric fields. The α_1 peak was observed only when the samples were

Table 1 The activation energy for each peak of the TSC spectrum, in eV.

TiO ₂ contents [mol %]	E _f [kV/m]	Tr [°C]	Peak	Unit [eV]			
				γ	β	α_2	α_1
0	E _f		2	0.07	0.33	0.17	
			4	0.06	0.27	0.32	
			6	0.06	0.41		0.38
			2	0.06		0.24	
			4	0.05		0.32	
			6	0.02		0.44	1.15
0	Tr		-100			0.55	
			-50			0.15	
			0			0.31	0.94
			50	0.07		0.41	0.33
			100	0.09	0.29	0.31	
			2	0.17		0.65	
2	Tr		-100	0.02			
			-50	0.02			
			0	0.07		0.48	1.42
			50	0.08		0.59	0.69
			100	0.17			

formed at 6kV/m. The β peak was observed in the range of room temperature depending on forming electric field. The temperature at which appeared the γ and α_2 peaks remained constant. It seems that origin of γ , β and α_2 may be caused by the shallow trapped electron, donor in grain itself and trapped electron in surface state, respectively.

For ZnO varistors with TiO₂ samples (Fig. 4), the amplitude of the TSC at γ peak did not change compared to the samples without TiO₂. The magnitude of the TSC at β and α_2 peaks decreased and the magnitude of the TSC for α_1 increased. That has a great influence on the conductivity of the samples which is dominated by the magnitudes of the TSC at α_2 and α_1 peaks.

The increase of the leakage current in ZnO varistors with TiO₂ is responsible for α_2 and α_1 peaks of the TSC spectrum.

When the TiO₂ is added to the ZnO varistor, the number of donor ions increased, which caused an increase in the magnitude of the TSC at α_1 peak. The increase of donor ions is affected by the radicals of Ti⁴⁺ which have more ions than radicals of Zn²⁺.

Fig. 5 presents the TSC spectrum when the samples were formed at temperature -100°C, 0°C, 50°C and 100°C during 5min, and at the forming electric field of 6kV/m.

For higher forming temperature, the magnitude of TSC at α_2 peak is higher and the α_2 peak appeared at lower temperature. The α_2 peak may be originated by detrapping the electrons deeply trapped at the inner surface level because it has higher activation energy. The γ peak may be created by detrapping of trapped electron in the surface level near the conduction band of the ZnO grains and the intergranular layers electrons in a donor level or within the depletion layer. The α_1 peak was observed at temperature around 160°C and appeared only when the forming temperature was 0°C or 50°C. For higher forming temperature, the magnitude of TSC at the α_1 peak is higher, and the peak appeared at the same temperature. The origin of the α_1 peak may be caused due to depolarization of donor ions in the depletion layer

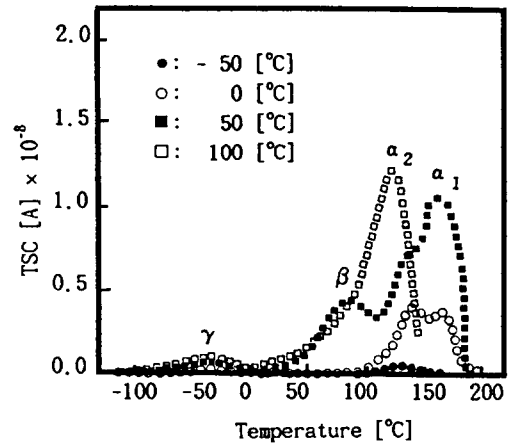


Fig. 5 TSC spectrum of ZnO varistors without TiO₂, forming electrical field:6(V), various forming temperature: -100, -50, 0, 50, 100[°C], forming time:5(min.), rising time:5[°C/min.]

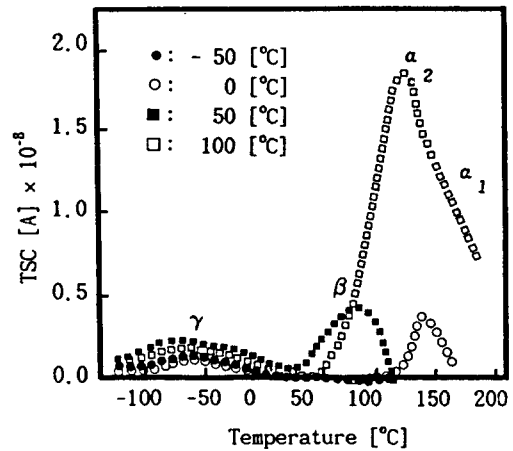


Fig. 6 TSC spectrum of ZnO varistors with TiO₂ 2 mol%, forming electrical field:6(V), various forming temperature: -100, -50, 0, 50, 100[°C], forming time:5(min.), rising time:5[°C/min.]

because the activation energy of ions is higher than that of electrons.

Hayashi et al[6] also observed the γ , β and α_1 peaks of the TSC spectrum for the ZnO varistor even without applying the

forming electric field.

The α_1 peak of the TSC spectrum was explained in paper[6] as due to the mobile ions.

Fig.6 presents the TSC spectrum for samples with TiO₂ mol%, formed at these same conditions as samples without TiO₂(Fig.5). For samples with TiO₂, the magnitude of TSC is higher than for samples without TiO₂. Therefore, it may be concluded that the α_2 and α_1 peaks of the TSC spectrum were created by the detrapping of trapped electrons and depolarization of donor ions.

Fig.7 presents the trap model of charged particles in the ZnO varistor and shows at which level appeared the γ , β , α_2 and α_1 peaks of the TSC spectrum.

- A : The origin of α_1 peak
- B : The origin of α_2 peak
- C : The origin of β peak
- D : The origin of γ peak

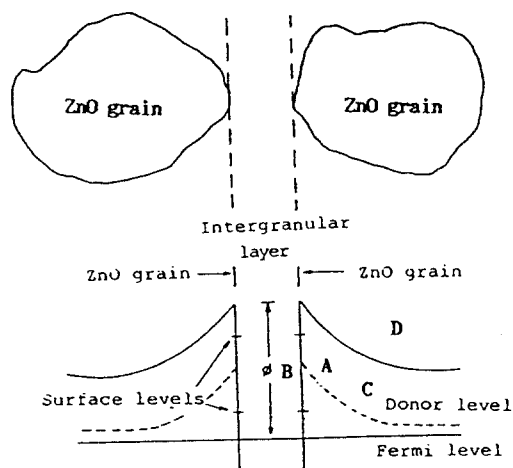


Fig.7 The band diagrams at the grain boundary region of ZnO varistors

4. Conclusions

As a result, investigation of the degradation mechanism of ZnO varistor fabricated with TiO₂ additions may be concluded as follows:

1. The origin of α_1 peak may be created by the thermal excitation of space charge formed in depletion layer. The

energy of thermal excitation for the space charge is about 0.33~1.42 eV.

2. The α_2 peak may be caused by the detrapping of trapped carriers in the surface state of grain boundary interface between the intergranular layer and ZnO grain.
3. The β peaks may be due to detrapping of trapped electrons in donor level of ZnO grains. Calculated donor level is about 0.3 eV.
4. The γ peak may be originated by the detrapping of impurity distributed within the bulk and trapped electrons in shallow trap.
5. The conduction properties of ZnO varistor may be determined by the height of α_1 and α_2 peak.

5. References

- [1] K. Eda, Iga and M. Matsuoka, "Degradation Mechanism of Non-Ohmic Zinc Oxide Ceramics", J. Appl. Phys., 51, No. 5, pp. 5754~5762, 1980.
- [2] Philipp H. R. and Levinson L. M., "Degradation Phenomena in Zinc Oxide Varistors", A Review Advances in Ceramics, Vol. 7, Am. Cer. Soc., pp. 1, 1983.
- [3] Sato K. and Takana Y., "A Mechanism of Degradation in Leakage Currents Through ZnO Varistors", J. Appl. Phys., Vol. 51, pp. 8819, 1982.
- [4] Eda K., and Iga A., "Degradation Mechanism of Non-Ohmic Zinc Oxide Ceramics", J. Appl. Phys., Vol. 51, p. 2678, 1980.
- [5] Creswell R. A., Perlman M. M., "Thermal Currents from Corona Charged Mylar", J. Appl. Phys., Vol. 41, p. 2365, 1970.
- [6] Masahiko Hayashi, Masanori Haba, Shinji Hirano, Masako Okamoto, and Misuzu Watanabe, "Degradation Mechanism of Zinc Oxide Varistors Under DC Bias", J. Appl. Phys., 53, No. 8, pp 5754~5762, 1982.
- [7] E. Olsson, G. L. Dunlop and R. Osterlund, "The Development of Interfacial Microstructure in a ZnO Varistor Material", J. Appl. Phys., 66(10) pp 5072-77(1989)
- [8] Deltlev F. K. Hennings, Ruediger Hertung, Piet J. L. Reijnen, "Grain Size Control in Low-Voltage Varistors", J. Am. Ceram.

Soc., 73(3) pp 645-648, (1990)
 [9] Taro Hino Kenji Suzuki and Ken Yamashita, "A Measurement of Relaxation Time of Dipole and Dielectric Loss Factor in Very Low Frequency by Thermally

Stimulated Current", Jap. J. Appl. Phys., 12[5] pp. 651-656, (1973)
 [10] IEEEJ, "電氣絶縁材料の熱刺激電流", 電氣學會 技術報告, 2 [194], PP. 53-68, (1985)

著者紹介



장경욱
 1963년 8월 27일생
 1986년 2월 광운대 전기공학과 졸업.
 1988년 9월 광운대 전기공학과 석사.
 1993년 현재 광운대 전기공학과 박사과정수료.



이준웅
 1940년 10월 24일생. 1964년 2월 한양대 전기공학과 졸업. 1970년 2월 한양대 전기공학과 석사. 1979년 3월 France국립 Montpellier 전기공학과(공박) 1990년 1-12월 미국 미시시피 주립대 교환교수. 1993년 현재 광운대 전기공학과 교수.



이성일
 1961년 7월 7일생. 1983년 2월 광운대 전기공학과 졸업. 1986년 2월 광운대 전기공학과(석사). 1988년 3월 현재 광운대 전기공학과 박사과정. 1992년 4월-93년 2월 충주공업전문대학 산업대 안전과 전임강사. 1993년 현재 충주산업대학 산업안전공학과 전임강사.